Dalton Transactions

PAPER

View Article Online
View Journal

Cite this: DOI: 10.1039/c8dt01871e

Preparation and reactivity of half-sandwich dioxygen complexes of ruthenium†

Gabriele Albertin, *[a] Stefano Antoniutti, [a] Marco Bortoluzzi, [a] Jesús Castro [b] and Valentina Ferraro[a]

Received 9th May 2018,
Accepted 19th June 2018

DOI: 10.1039/c8dt01871e

rsc.li/dalton

Dioxygen complexes [Ru(η^5-C_5Me_5)(η^2-O_2){P(OEt)$_3$}$_2$]BPh$_4$ (**1**) and [Ru(η^5-C_5Me_5)(η^2-O_2)(PPh$_3$){P(OR)$_3$}]BPh$_4$ (**2**, **3**) [R = Me (**2**), Et (**3**)] were prepared by allowing chloro-complexes RuCl(η^5-C_5Me_5)[P(OEt)$_3$]$_2$ and RuCl(η^5-C_5Me_5)(PPh$_3$)[P(OR)$_3$] to react with air (1 atm) in the presence of NaBPh$_4$. Substitution of the η^2-O_2 in **1–3** by alkenes [CH$_2$=CH$_2$, CH=CHCO(O)CO] and terminal alkynes (PhC≡CH) afforded [Ru(η^5-C_5Me_5)(η^2-CH$_2$=CH$_2$){P(OEt)$_3$}L]BPh$_4$ (**4**) [L = P(OEt)$_3$ (a), PPh$_3$ (b)], [Ru(η^5-C_5Me_5){η^2-CH=CHCO(O)CO}{P(OEt)$_3$}$_2$]BPh$_4$ (**5**) and [Ru(η^5-C_5Me_5){=C=C(H)Ph}{P(OEt)$_3$}$_2$]BPh$_4$ (**6**) derivatives. Protonation of dioxygen complexes **1–3** with triflic acid yielded phosphate complexes [Ru(κ^1-OTf)(η^5-C_5Me_5){P(O)(OEt)$_3$}$_2$] (**7**) and [Ru(κ^1-OTf)(η^5-C_5Me_5){P(O)Ph$_3$}{P(O)(OMe)$_3$}] (**8**). A reaction path for the formation of complexes **7** and **8** is proposed by DFT studies. Besides phosphate complex **7**, protonation of **1** under a CH$_2$=CH$_2$ atmosphere (1 atm) afforded acetic acid. Treatment of complexes **7** and **8** with ^{t}BuNC afforded the tris(isocyanide) derivative [Ru(η^5-C_5Me_5)(^{t}BuNC)$_3$]BPh$_4$ (**9**). The complexes were characterised spectroscopically (IR and NMR) and by X-ray crystal structure determination of **1**, **2** and **3**.

Introduction

The activation of dioxygen by transition metal fragments has attracted considerable attention in recent decades because of its relevance to biological oxidation reactions[1] and interest for its application in industrial processes.[2] Although the latter often exploit partially-reduced forms of O_2, such as peroxides or oxo-complexes,[2] nature operates with the most readily-available oxidant, *i.e.*, dioxygen, using metal complexes having a d^6 configuration as catalysts.[3]

In this context, a number of transition metal complexes containing dioxygen as a ligand (η^2-O_2) were prepared[4,5] and some studies on the oxygen transfer reaction reported.[4,5] The principal type involves the iron triad as a central metal with bidentate phosphine or cyclopentadienyl as supporting ligands.[4g–o,q,5a,d,i] The activation of dioxygen by these fragments often involves the formation of oxo complexes [M]=O as intermediates,[3,4k,n] relevant in olefin epoxidation[6] and alkene hydroxylation reaction.[7] Examples of intramolecular dioxygen transfer to organic substrates are also reported.[4b,l,i]

We are interested in the chemistry of half-sandwich complexes of ruthenium with phosphite ligands[8] and have recently reported[9,10] that the cyclopentadienyl and pentamethylcyclopentadienyl fragments [Ru(η^5-C_5H_5)(PPh$_3$){P(OR)$_3$}]$^+$ and [Ru(η^5-C_5Me_5)(L){P(OR)$_3$}]$^+$ [L = PPh$_3$, P(OR)$_3$] show interesting properties in the activation of coordinate diazoalkane towards both (3 + 2) cycloaddition[9] and hydrolysis reactions.[10] These results prompted us to extend our studies on half-sandwich complexes to dioxygen in order to test whether η^2-O_2 complexes may form and how these fragments may activate this important molecule. The results of these studies are reported here.

Results and discussion

Preparation of η^2-O_2 derivatives

Dioxygen complexes of ruthenium of the types [Ru(η^5-C_5Me_5)(η^2-O_2){P(OEt)$_3$}$_2$]BPh$_4$ (**1**) and [Ru(η^5-C_5Me_5)(η^2-O_2)(PPh$_3$){P(OR)$_3$}]BPh$_4$ (**2**, **3**) [R = Me (**2**), Et (**3**)] were prepared by allowing either the chloro-complex RuCl(η^5-C_5Me_5)[P(OEt)$_3$]$_2$ or RuCl(η^5-C_5Me_5)(PPh$_3$)[P(OR)$_3$] to stir under air (1 atm) in the presence of NaBPh$_4$, as shown in Scheme 1.

The reaction proceeds with substituting the Cl$^-$ ligand and forming dioxygen complexes **1–3**, which were separated as BPh$_4$ salts and characterised. Crucial for successful syntheses was the presence of the salt NaBPh$_4$, which, favoured the substitution of the Cl$^-$ ligand and allowed the complexes to separate as solids in good yields.

[a]*Dipartimento di Scienze Molecolari e Nanosistemi, Università Ca' Foscari Venezia, Via Torino 155, 30172 Venezia Mestre, Italy. E-mail: albertin@unive.it*
[b]*Departamento de Química Inorgánica, Universidade de Vigo, Facultade de Química, Edificio de Ciencias Experimentais, 36310 Vigo, Galicia, Spain*

† Electronic supplementary information (ESI) available. CCDC 1842088–1842090. For ESI and crystallographic data in CIF or other electronic format see DOI: 10.1039/c8dt01871e

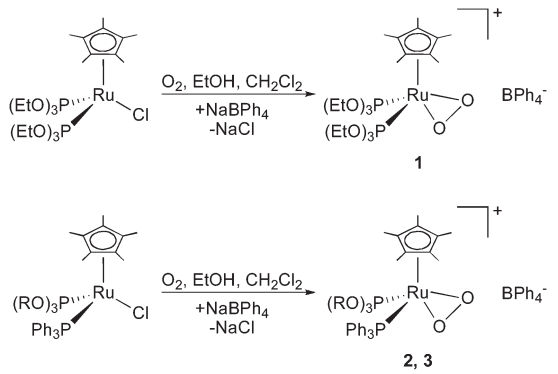

Scheme 1 R = Me (**2**), Et (**3**).

Both the bis(phosphite) $[Ru(\eta^5\text{-}C_5Me_5)\{P(OEt)_3\}_2]^+$ and mixed-ligand $[Ru(\eta^5\text{-}C_5Me_5)(PPh_3)\{P(OR)_3\}]^+$ fragments were able to coordinate the dioxygen molecule, affording yellow-orange solids **1–3**, stable in air and in solution of polar organic solvents, where they behaved as 1 : 1 electrolytes.[11]

Analytical and spectroscopic data (IR and NMR) confirmed the proposed formulation, which was further supported by X-ray crystal structure determination of $[Ru(\eta^5\text{-}C_5Me_5)(\eta^2\text{-}O_2)\{P(OEt)_3\}_2]BPh_4$ (**1**), $[Ru(\eta^5\text{-}C_5Me_5)(\eta^2\text{-}O_2)(PPh_3)\{P(OMe)_3\}]BPh_4$ (**2**) and $[Ru(\eta^5\text{-}C_5Me_5)(\eta^2\text{-}O_2)(PPh_3)\{P(OEt)_3\}]BPh_4$ (**3**).

The three complexes consist of tetraphenylborate salts of ruthenium complexes. Only the corresponding cation of **2** is shown in Fig. 1. This is because the other compounds differ only in phosphorus donors, *i.e.*, **1** contains two phosphite ligands $P(OEt)_3$ and **3** contains one $P(OEt)_3$ and one PPh_3 ligand.

In all cases, the cation complex contains a ruthenium atom in a half-sandwich piano-stool structure, coordinated by a pentamethylcyclopentadienide group (Cp*), the two above-mentioned phosphine ligands and a dioxygen ligand in a η^2 coordination manner, also called side-on behaviour. The overall geometry of the complex is pseudo octahedral, where three of the positions are occupied by the Cp* ligand and the dioxygen donor ligand occupies only one of the coordination sites. In this way, the angles between the legs (see Table 1) are near 90°. The P–Ru–P angles are between 85.207(12)° and 88.024(13)°, and the other angles to be considered are those between the centre of the O–O bond and the phosphorus atom, P–Ru–Ct2 angles. These, probably due to sterical reasons, are bigger, between 95.639(10)° and 101.837(11)°. The Ru–P bond lengths depends on the nature of the ligand, with values around 2.28 Å for phosphite ligands and about 2.37 Å for triphenylphosphine ligands. Coordination of the Cp* ligand also shows the small differences depending on the phosphorus ligands, so the Ru–C bond average is about 2.27 Å for mixed ligands and slightly shorter for the diphosphite compound. It is worth noting that these parameters are very similar to those found in other Ru(II) compounds previously described by our group.[10b,c] The dioxygen ligand is situated in a side-on mode, with Ru–O bond distances between 2.0207(9) and 2.2939(4) Å. However, the distance between the metal atom and the middle of the O–O bond (Ru–Ct2 entry in Table 1) does not depend on the ancillary ligand. The O–O bond distance is between 1.401(3) and 1.4104(13) Å. These features have also been found in several similar compound with the $Cp^*Ru(O_2)P1P2$ moiety previously, where P1 and P2 are different phosphorus donors.[4i,l,o,s,t,5d,13–15] Worthy of note is that, in literature, the compounds are discussed as formally Ru(IV)-peroxo complexes, since the O–O bond distance is in the middle of the wide range found in classical peroxo compounds such as potassium peroxide or hydrogen peroxide.[4t]

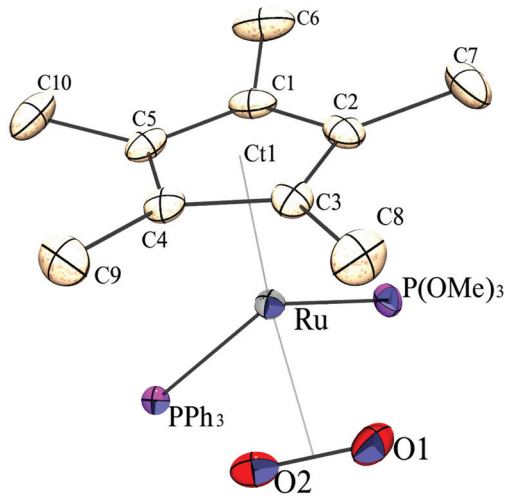

Fig. 1 ORTEP[12] view of the cation in the compound $[Ru(\eta^5\text{-}C_5Me_5)(\eta^2\text{-}O_2)(PPh_3)\{P(OMe)_3\}]BPh_4$ (**2**).

Table 1 Selected bond lengths [Å] and angles [°]

	1	2	3
Ru–CT1	1.89329(17)	1.9132(3)	1.9140(6)
Ru–CT2	1.90535(14)	1.9039(2)	1.9041(7)
Ru–O(1)	2.0342(9)	2.0366(17)	2.0207(9)
Ru–O(2)	2.0270(9)	2.0211(17)	2.0404(9)
Ru–P(1)	2.2801(4)	2.2895(6)	2.2939(4)
Ru–P(2)	2.2752(3)	2.3752(6)	2.3727(4)
Ru–C(1)	2.2553(12)	2.252(2)	2.2428(13)
Ru–C(2)	2.2845(12)	2.229(2)	2.3025(13)
Ru–C(3)	2.2839(13)	2.236(2)	2.3092(13)
Ru–C(4)	2.2469(12)	2.296(2)	2.2636(13)
Ru–C(5)	2.2126(12)	2.316(2)	2.2325(13)
$Ru\text{–}C_{av}$	2.2568	2.266	2.2701
O(1)–O(2)	1.4045(13)	1.401(3)	1.4104(13)
CT1–Ru–CT2	125.021(6)	121.110(10)	120.182(7)
CT1–Ru–P(1)	119.886(9)	119.976(18)	119.992(11)
CT1–Ru–P(2)	124.527(10)	128.638(16)	129.292(10)
CT2–Ru–P(1)	95.639(10)	100.642(19)	101.837(11)
CT2–Ru–P(2)	94.595(10)	91.830(16)	92.125(10)
P(1)–Ru–P(2)	88.024(13)	86.22(2)	85.207(12)

CT1 is the centroid of the Cp* ligand. CT2 is the centroid of the O_2 ligand.

In the IR spectrum of **1** a weak band assignable to ν_{O-O} was observed at 935 cm^{-1}, which is absent in the spectrum of the precursor $RuCl(\eta^5\text{-}C_5Me_5)[P(OEt)_3]_2$. In the related complexes **2** and **3** this ν_{O-O} band is not unambiguously assignable.

The proton NMR spectra of dioxygen complexes **1–3** show the signals of the $\eta^5\text{-}C_5Me_5$ ligand methyl substituents as either a triplet (**1**) or a doublet (**2**, **3**), owing to coupling with the P nuclei of $P(OR)_3$ phosphites. The characteristic signals of phosphine PPh_3, phosphites and of the BPh_4^- anion also appear in the spectra, whereas the ^{31}P NMR spectra are a singlet for **1** and an AX quartet for **2** and **3**, fitting the proposed formulation for the dioxygen derivatives.

DFT calculations on the cation $[Ru(\eta^5\text{-}C_5Me_5)(\eta^2\text{-}O_2)\{P(OMe)_3\}_2]^+$ support the idea that these compounds are better described as Ru(IV) peroxo-complexes rather than Ru(II) dioxygen derivatives. Both the π^* orbitals of coordinated $[O_2]$ are doubly occupied, that of the highest-energy (HOMO) behaving as non-bonding with respect to $[Ru–O_2]$ interaction. Instead, the other π^* orbital is involved in σ-interactions with the metal centre, mainly described by HOMO−2 and HOMO−7 orbitals. The interaction of the $[O_2]$ fragment with ruthenium is supported by the overlap of the occupied O_2 π-orbitals with those of the $[Ru(\eta^5\text{-}C_5Me_5)\{P(OMe)_3\}_2]^+$ cation as is observable, for instance, in HOMO−36, HOMO−38 and HOMO−42 MOs (Fig. 2). The negative Hirshfeld charge on coordinated $[O_2]$, −0.39 a.u., is in agreement with the formal formation of peroxo-derivatives. It is worth noting that the Hirshfeld charge on the metal centre, 0.29 a.u., is quite similar to the value calculated for the Ru(II) bis-organophosphate derivative $[Ru(\eta^5\text{-}C_5Me_5)\{P(O)(OMe)_3\}_2]^+$, 0.32 a.u. (*vide infra*), highlighting that formal changes in the oxidation state of the ruthenium centre are compensated by the ancillary ligands.

Reactivity

Reactivity studies of our dioxygen complexes **1–3** with alkenes and alkynes were undertaken with the aim of testing whether the transfer of dioxygen to the organic substrate is possible. The results show that, at room temperature, complexes **1–3** do not react with alkene [$CH_2{=}CH_2$, $\overline{CH{=}CHCO(O)CO}$] and alkyne (PhC≡CH), leaving the starting complexes unchanged after 48 h of reaction. Instead, in refluxing 1,2-dichloroethane, $\eta^2\text{-}O_2$ was substituted, affording η^2-alkene $[Ru(\eta^5\text{-}C_5Me_5)(\eta^2\text{-}CH_2{=}CH_2)\{P(OEt)_3\}L]BPh_4$ (**4**), $[Ru(\eta^5\text{-}C_5Me_5)\{\eta^2\text{-}\overline{CH{=}CHCO(O)CO}\}\{P(OEt)_3\}_2]BPh_4$ (**5**) and vinylidene $[Ru(\eta^5\text{-}C_5Me_5)\{{=}C{=}C(H)Ph\}\{P(OEt)_3\}_2]BPh_4$ (**6**) derivatives, which can be isolated and characterised (Scheme 2).

The reaction seems to only involve the substitution of the $\eta^2\text{-}O_2$ ligand by the unsaturated organic substrate, because no evidence of oxidation products was detected in the reaction mixture, but only in the excess of organic reagents.

The stability of the $\eta^2\text{-}O_2$ ligand and the related absence of oxygen-transfer reactions prompted us to study the behaviour of the $\eta^2\text{-}O_2$ species in the presence of Brønsted acids. We began with the reaction of **1–3** with HOTf at low temperature, adding increasing amounts of acid to a CD_2Cl_2 solution and monitoring the progress of the reaction by NMR spectra. The results showed that adding HOTf to $[Ru(\eta^5\text{-}C_5Me_5)(\eta^2\text{-}O_2)\{P(OEt)_3\}_2]BPh_4$ (**1**) caused the disappearance of the singlet at 117.0 ppm of the $P(OEt)_3$ and the appearance of a new singlet at −2.77 ppm in the ^{31}P spectrum, attributed to the coordinated triethylphosphate $P(O)(OEt)_3$ of a new species that was formed. Apart from the signals of the starting complex **1** and of the phosphate, no other signals appeared both in the ^1H and ^{31}P NMR spectra, preventing the identification of other

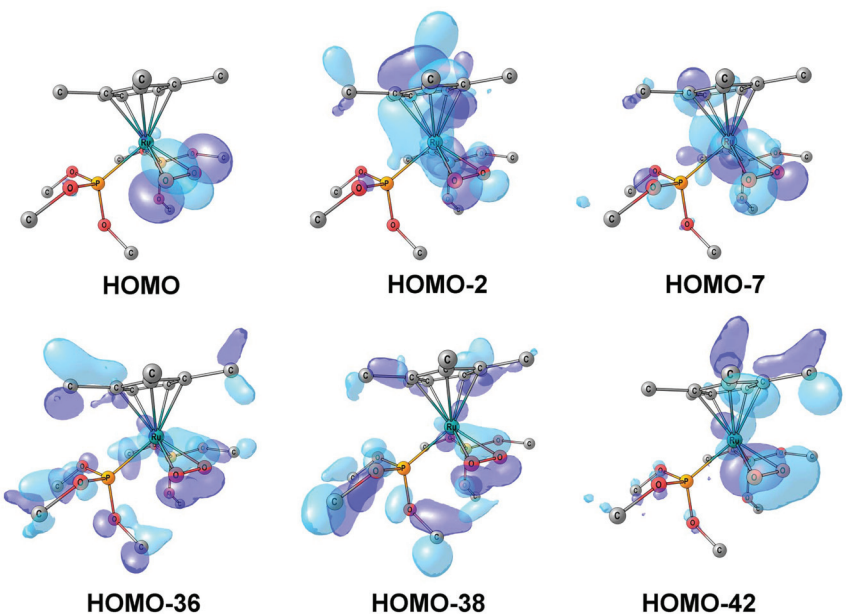

Fig. 2 Selected occupied MOs of $[Ru(\eta^5\text{-}C_5Me_5)(\eta^2\text{-}O_2)\{P(OMe)_3\}_2]^+$. C-PCM/ωB97X calculations. Hydrogen atoms are omitted for clarity. Surface isovalue = 0.04 a.u.

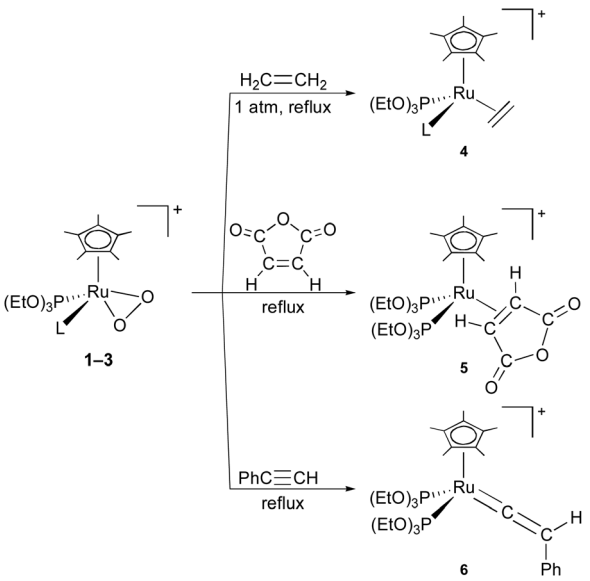

Scheme 2 L = $P(OEt)_3$ (a), PPh_3 (b).

intermediates. We attempted to isolate the formed complexes, but only an oil was isolated, the NMR spectra of which agree with the presence of a bis(phosphate) complex of the type $[Ru(\kappa^1\text{-OTf})(\eta^5\text{-}C_5Me_5)\{P(O)(OEt)_3\}_2]$ (**7**) (Scheme 3).

The $P(O)(OEt)_3$ ligand can be removed from complex **7** by substitution with ^{t}butylisocyanide (Scheme 4) and chromatographic separation.

The NMR spectrum supports the proposed formulation when compared with an authentic sample of $P(O)(OEt)_3$, suggesting the coordination of $P(O)(OEt)_3$ in complex **7**. On this basis, we can hypothesise that the acid promotes oxygen-transfer to each phosphorus atom of the phosphite, affording two phosphate molecules $P(O)(OEt)_3$, which can O-coordinate to the metal centre, affording the $[Ru(\kappa^1\text{-OTf})(\eta^5\text{-}C_5Me_5)\{P(O)(OEt)_3\}_2]$ (**7**) derivative.

The protonation reaction of $[Ru(\eta^5\text{-}C_5Me_5)(\eta^2\text{-}O_2)\{P(OEt)_3\}_2]^+$ (**1**) in CD_2Cl_2 was also tested with $HBF_4{\cdot}Et_2O$ and in this case the NMR spectra also indicated the formation of the phosphate $P(O)(OEt)_3$. Nonetheless, the complex obtained was not stable and in few minutes decomposed releasing the phosphate. This different behaviour may still be explained on the basis of an initial protonation of the $\eta^2\text{-}O_2$, which promotes the oxygen transfer to $P(OEt)_3$ affording the phosphate species $P(O)(OEt)_3$. However, the instability of the formed complex, *i.e.*, $[Ru(\eta^5\text{-}C_5Me_5)\{P(O)(OEt)_3\}_2]^+$, may be attributed to the poor coordinating properties of the BF_4^- anion, which is not able to stabilise the species $[Ru(\kappa^1\text{-}BF_4)(\eta^5\text{-}C_5Me_5)\{P(O)(OEt)_3\}_2]$ which could be formed. Support for this hypothesis came from the use of CF_3COOH, the reaction of which with $[Ru(\eta^5\text{-}C_5Me_5)(\eta^2\text{-}O_2)\{P(OEt)_3\}_2]^+$ gave a stable oily product formulated by NMR as $[Ru(\kappa^1\text{-}OCOCF_3)(\eta^5\text{-}C_5Me_5)\{P(O)(OEt)_3\}_2]$ (**7′**). The use of a Brønsted acid containing a good coordinating anion (OTf^- or CF_3COO^-) allowed the stabilisation of the phosphate complex **7** or **7′** which, unfortunately, can only be separated as an oil.

Mixed-ligand dioxygen complex $[Ru(\eta^5\text{-}C_5Me_5)(\eta^2\text{-}O_2)(PPh_3)\{P(OMe)_3\}]BPh_4$ (**2**) also reacts in the presence of HOTf to afford the phosphine oxide-phosphate compound of the type $[Ru(\kappa^1\text{-OTf})(\eta^5\text{-}C_5Me_5)\{P(O)Ph_3\}\{P(O)(OMe)_3\}]$ (**8**) (Scheme 5).

Following the progress of the protonation reaction by ^{31}P NMR spectra, we observed the disappearance of the AX quartet of the dioxygen precursor **2** and the appearance of two singlets at 30.5 and 0.47 ppm, attributed to phosphine oxide $P(O)(Ph)_3$ and phosphate $P(O)(OMe)_3$, respectively, bonded to the central metal. The formation of phosphine oxide and phosphate from the oxidation of coordinated phosphine by $\eta^2\text{-}O_2$ was confirmed by substituting both $P(O)(Ph)_3$ and $P(O)(OMe)_3$ groups from compound **8** with ^{t}BuNC, obtaining compound **9**. The ^{1}H and ^{31}P NMR spectra confirmed the proposed formation of the species $P(O)(Ph)_3$ and $P(O)(OMe)_3$ when compared with the spectra of authentic samples. In addition, a comparison between the spectra of $[Ru(\kappa^1\text{-OTf})(\eta^5\text{-}C_5Me_5)\{P(O)Ph_3\}\{P(O)(OMe)_3\}]$ (**8**) and of free phosphine oxide and phosphate suggested the O-coordination of both $P(O)(Ph_3)$ and $P(O)(OMe)_3$ species. However, even at −90 °C, the ^{31}P NMR spectra of **8** appear as two singlets, indicating that the ^{31}P coupling between the two species $P(O)(Ph)_3$ and $P(O)(OMe)_3$, is so small as to result

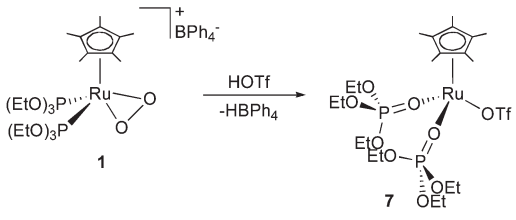

Scheme 3

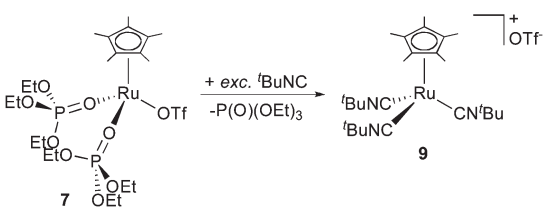

Scheme 4

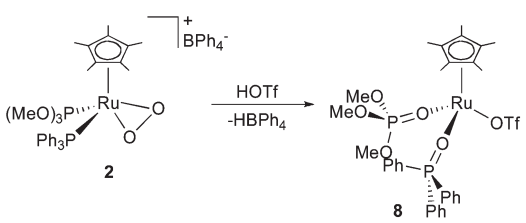

Scheme 5

undetectable. It is probable that an exchange process still occurs even at this temperature, preventing the detection of the expected ^{31}P–^{31}P coupling.

Acid-promoted oxygen transfer has been proposed for several peroxo complexes,[1,4a,b,n,16] whereas intramolecular η^2-O_2 transfer to coordinate phosphine is very rare[4i,l] and seems to involve hydroperoxide intermediates. A plausible mechanism for the intramolecular oxidation of coordinated phosphines is depicted in Scheme 6 (black path), where $[Ru(\eta^5\text{-}C_5Me_5)(\eta^2\text{-}O_2)\{P(OMe)_3\}_2]^+$ and HBF_4 are viewed as reactants (**R**). DFT C-PCM/ωB97X calculations allow to optimise possible intermediates of the reaction affording the corresponding bis(phosphate) complex as the final product.

Protonation of the coordinated $[O_2]$ fragment affording the intermediate species $\mathbf{I_1}$ is a favourable process, the associated Gibbs energy variation being −16.9 kcal mol^{-1}. Such a result is in agreement with the previously described peroxo-character of the coordinated O_2 ligand. The compound $[Ru(\eta^5\text{-}C_5Me_5)(\eta^2\text{-}O_2H\cdots BF_4)\{P(OMe)_3\}_2]^+$ ($\mathbf{I_1}$) has singlet multiplicity. As depicted in Scheme 6, the O_2-ligand keeps the η^2 coordination mode after protonation, the computed Ru–OH bond length being only 0.174 Å longer than the Ru–O one (2.188 and 2.014 Å, respectively). The possible change of multiplicity of the complex after protonation was ruled out, being $[Ru(\eta^5\text{-}C_5Me_5)(\eta^2\text{-}O_2H\cdots BF_4)\{P(OMe)_3\}_2]^+$ in triplet state ($\mathbf{I_1^t}$, sketched in red in Scheme 6) less stable than $\mathbf{I_1}$ by about 15.8 kcal mol^{-1}.

The first oxygen transfer to one of the phosphine ligands could involve the protonated oxygen atom of the $[O_2H\cdots BF_4]$ moiety, affording the oxo-complex $\mathbf{I_2^{oxo}}$ (sketched in red in Scheme 6), or the non-protonated oxygen, with the formation of the hydroxo-intermediate $\mathbf{I_2}$. This last possibility is more favourable from a thermodynamic point of view, being $[Ru(\eta^5\text{-}C_5Me_5)(OH\cdots BF_4)\{P(OMe)_3\}\{P(O)(OMe)_3\}]^+$ ($\mathbf{I_1}$) more stable than the oxo-species $\mathbf{I_2^{oxo}}$ by about 6.5 kcal mol^{-1}. Moreover, the trimethylphosphate ligand dissociates as $P(O)(OMe)_3{\cdot}HBF_4$ from the oxo-intermediate $\mathbf{I_2^{oxo}}$, while it remains coordinated in the hydroxo-complex $\mathbf{I_2}$. In any case, the processes involving the break of the O–O bond and the consequent formation of a P=O bond are characterised by high negative ΔG variations, −58.2 kcal mol^{-1} where $\mathbf{I_2}$ is considered as an intermediate. Therefore, the relative slowness of the reaction (*vide infra*) is probably associated to high-energy transition states. In fact, DFT calculations for oxygen transfer carried out at EDF2 level permitted the finding of a coherent transition state geometry (**TS**, imaginary frequency = i569 cm^{-1}) and the estimation of the energy barrier around 32 kcal mol^{-1}.

The formation of the second organophosphate ligand from $\mathbf{I_2}$ is another thermodynamically favourable process, the associated ΔG being around −19.0 kcal mol^{-1}. The product

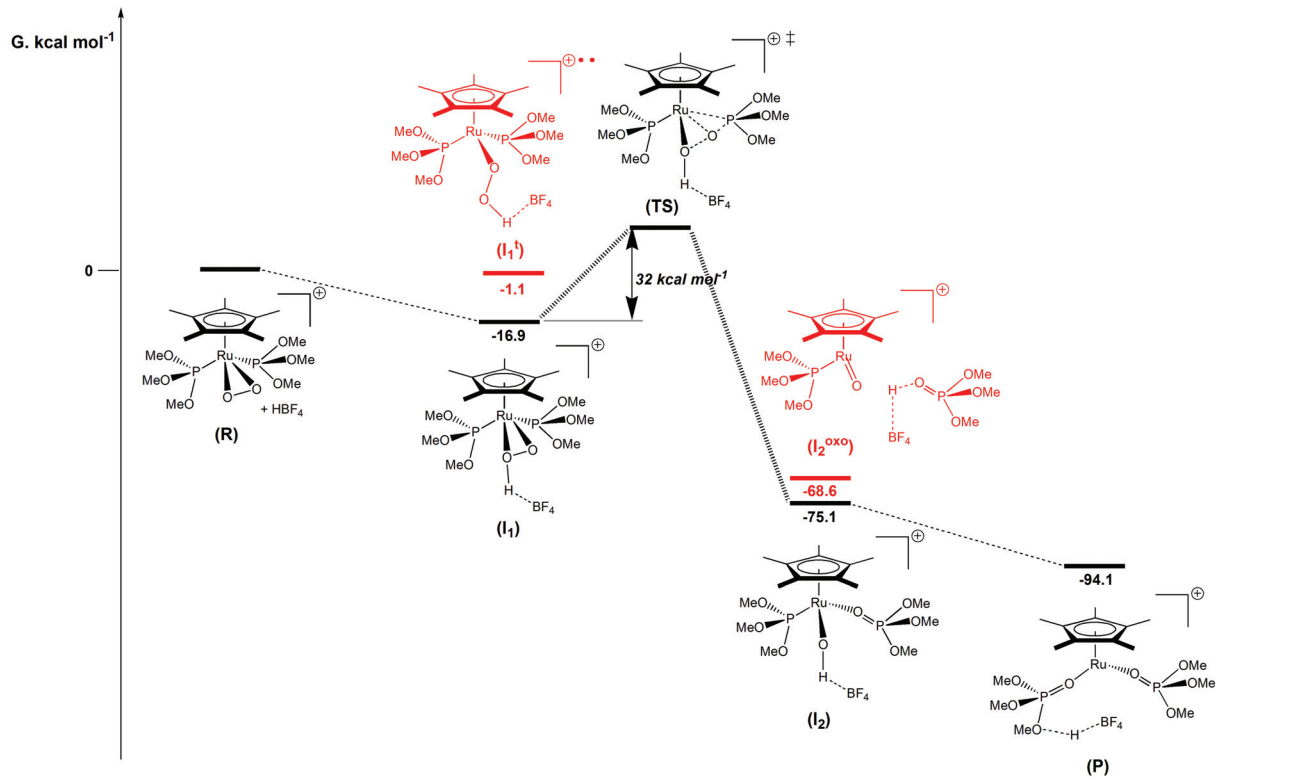

Scheme 6 DFT-optimised intermediates proposed for the reaction of $[Ru(\eta^5\text{-}C_5Me_5)(\eta^2\text{-}O_2)\{P(OMe)_3\}_2]^+$ with HBF_4 (**R**) affording $[Ru(\eta^5\text{-}C_5Me_5)\{P(O)(OMe)_3\}\{P(O)(OMe)_3\cdots HBF_4\}]^+$ (**P**). C-PCM/ωB97X calculations, dichloromethane as continuous medium. Relative Gibbs free energies in kcal mol^{-1}. Black path: Lowest-energy reaction pathway. Selected higher energy intermediates are depicted in red. Energy barrier for the oxygen transfer calculated at DFT C-PCM/EDF2 level. Pictures and Cartesian coordinates of the DFT-optimised geometries are collected in ESI.†

$[Ru(\eta^5\text{-}C_5Me_5)\{P(O)(OMe)_3\}\{P(O)(OMe)_3\cdots HBF_4\}]^+$ (**P**) is coordinatively unsaturated and HBF_4 interacts with one of the [OMe] substituents. It is likely that the use of more coordinating counter-anions, such as triflate or trifluoroacetate, affords more stable products.

The acid-catalysed oxidation of coordinated phosphines in our η^2-O_2 complex $[Ru(\eta^5\text{-}C_5Me_5)(\eta^2\text{-}O_2)\{P(OEt)_3\}_2]BPh_4$ (**1**) to give phosphate is rather slow and the formation of $[Ru(\kappa^1\text{-}OTf)(\eta^5\text{-}C_5Me_5)\{P(O)(OEt)_3\}_2]$ (**7**) was almost completed only after 24 h. Such a slow intramolecular oxygen transfer prompted us to test whether other substrates, *e.g.*, alkenes, may be involved in oxygen transfer giving oxidised products. Because ethylene did not react at room temperature with $[Ru(\eta^5\text{-}C_5Me_5)(\eta^2\text{-}O_2)\{P(OEt)_3\}_2]BPh_4$, we treated the η^2-O_2 complex **1** in $CDCl_3$ first with $CH_2{=}CH_2$ (1 atm) and then with two equivalents of triflic acid. The progress of the reaction was monitored by NMR spectra, which showed that the addition of HOTf caused the disappearance of the signals of starting complex **1** and the formation of acetic acid CH_3COOH (Scheme 7), besides the known phosphate complex $[Ru(\kappa^1\text{-}OTf)(\eta^5\text{-}C_5Me_5)\{P(O)(OEt)_3\}_2]$ (**7**).

In the spectra, the signal of the known η^2-$CH_2{=}CH_2$ derivative $[Ru(\eta^5\text{-}C_5Me_5)(\eta^2\text{-}CH_2{=}CH_2)\{P(OEt)_3\}_2]^+$ (**4a**) also appeared. The formation of acetic acid is rather surprising and indicated that intermolecular oxygen transfer can also occur, giving oxidation products of the organic substrate present in the solution. Indeed, inter- and intramolecular processes are in competition, where a prevalence of the intramolecular gives phosphate. The ratio between complex **7** and acetic acid is about 6 : 1. The formation of acetic acid may tentatively be explained as being based on the protonation of ethylene by HOTf. This gives the carbocation $CH_2CH_3^+$, which behaves as an electrophile on the coordinated η^2-O_2 and gives a peroxo intermediate of the type [**C**] (Scheme 8). This intermediate may either give intramolecular oxygen transfer, affording phosphate complex **7**, or lose the ethylene peroxo species $\overline{CH_2\text{–}CH_2\text{–}O\text{–}O}$, which tautomerises giving acetic acid. In all cases and irrespective of the underlying mechanism, the formation of CH_3COOH indicates that our dioxygen complex **1** also behaves towards ethylene as an oxidising agent.

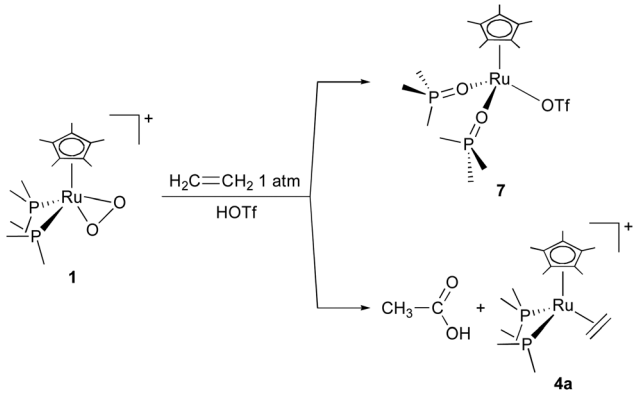

Scheme 7 P = $P(OEt)_3$

On this basis, we treated the complex $[Ru(\eta^5\text{-}C_5Me_5)(\eta^2\text{-}O_2)\{P(OEt)_3\}_2]BPh_4$ with a mixture of $CH_2{=}CH_2$ and O_2 (1 atm) and added triflic acid to test whether catalytic oxidation of ethylene may occur. Unfortunately, no catalytic cycle was observed and the amount of detected acetic acid was the same that was formed in the absence of O_2. This is probably due to the properties of the half-sandwich intermediate $[Ru(\kappa^1\text{-}OTf)(\eta^5\text{-}C_5Me_5)\{P(OEt)_3\}_2]^+$ **[D]** (Scheme 8), which exclusively gave the η^2-$CH_2{=}CH_2$ complex $[Ru(\eta^5\text{-}C_5Me_5)(\eta^2\text{-}CH_2{=}CH_2)\{P(OEt)_3\}_2]^+$ (**4a**) in the reaction with ethylene and molecular oxygen. The non-formation of the η^2-O_2 derivative $[Ru(\eta^5\text{-}C_5Me_5)(\eta^2\text{-}O_2)\{P(OEt)_3\}_2]^+$ (**1**), which should be the key intermediate in the catalytic cycle, prevents the further oxidation reaction. In fact, after adding the acid, the NMR spectra of the reaction mixture containing $[Ru(\eta^5\text{-}C_5Me_5)(\eta^2\text{-}O_2)\{P(OEt)_3\}_2]BPh_4$ and ethylene showed the formation of the ethylene complex $[Ru(\eta^5\text{-}C_5Me_5)(\eta^2\text{-}CH_2{=}CH_2)\{P(OEt)_3\}_2]BPh_4$ both in the absence and in the presence of free O_2, which prevents the activation by coordination of the dioxygen molecule in a catalytic oxidation process.

Characterisation of complexes

η^2-Alkene complexes $[Ru(\eta^5\text{-}C_5Me_5)(\eta^2\text{-}CH_2{=}CH_2)\{P(OEt)_3\}L]BPh_4$ (**4**), $[Ru(\eta^5\text{-}C_5Me_5)\{\eta^2\text{-}\overline{CH{=}CHCO(O)CO}\}\{P(OEt)_3\}_2]BPh_4$ (**5**) and the vinylidene derivative $[Ru(\eta^5\text{-}C_5Me_5)\{{=}C{=}C(H)Ph\}\{P(OEt)_3\}_2]BPh_4$ (**6**) were separated as yellow or orange solids, stable in air and in solution of polar organic solvents, where they behave as 1 : 1 electrolytes.[11] Analytical and spectroscopic data (IR and NMR) support the proposed formulation. Besides the signals of the ancillary ligands C_5Me_5 and $P(OEt)_3$ and of the BPh_4 anion, the ^{1}H NMR spectrum of the ethylene complex $[Ru(\eta^5\text{-}C_5Me_5)(\eta^2\text{-}CH_2{=}CH_2)\{P(OEt)_3\}_2]BPh_4$ (**4a**) shows one triplet at 3.05 ppm (J_{PH} = 3.5 Hz) due ethylene ligand protons. Instead, the spectrum of the related complex $[Ru(\eta^5\text{-}C_5Me_5)(\eta^2\text{-}CH_2{=}CH_2)\{P(OEt)_3\}(PPh_3)]BPh_4$ (**4b**) shows two multiplets, at 2.48 and 2.31 ppm, attributable to the η^2-$CH_2{=}CH_2$ ligand. Lowering the sample temperature caused some variations in the spectrum, but ethylene peaks are broad even at −90 °C, indicating that the rotation of $CH_2{=}CH_2$ still took place at this temperature. However, the RT pattern of the mixed-ligand compound **4b** can be simulated by an ABCDXY model (X, Y = ^{31}P) with the parameters listed in the Experimental section and the good fit between the calculated and experimental spectra strongly supports the proposed attribution. Similar behaviour has been observed in strictly-comparable complexes.[10c] In the temperature range between +20 and −80 °C, the ^{31}P NMR spectrum of the phosphite complex **4a** is a singlet at 131.5 ppm, whereas that of the mixed-ligand **4b** is an AX quartet, fitting the proposed formulation for the complexes.

The IR and NMR spectra of maleic anhydride $[Ru(\eta^5\text{-}C_5Me_5)\{\eta^2\text{-}\overline{CH{=}CHCO(O)CO}\}\{P(OEt)_3\}_2]BPh_4$ (**5**) and vinylidene derivative $[Ru(\eta^5\text{-}C_5Me_5)\{{=}C{=}C(H)Ph\}\{P(OEt)_3\}_2]BPh_4$ (**6**) are exactly the same of the sample previous reported by us[10c] and will not be discussed further.

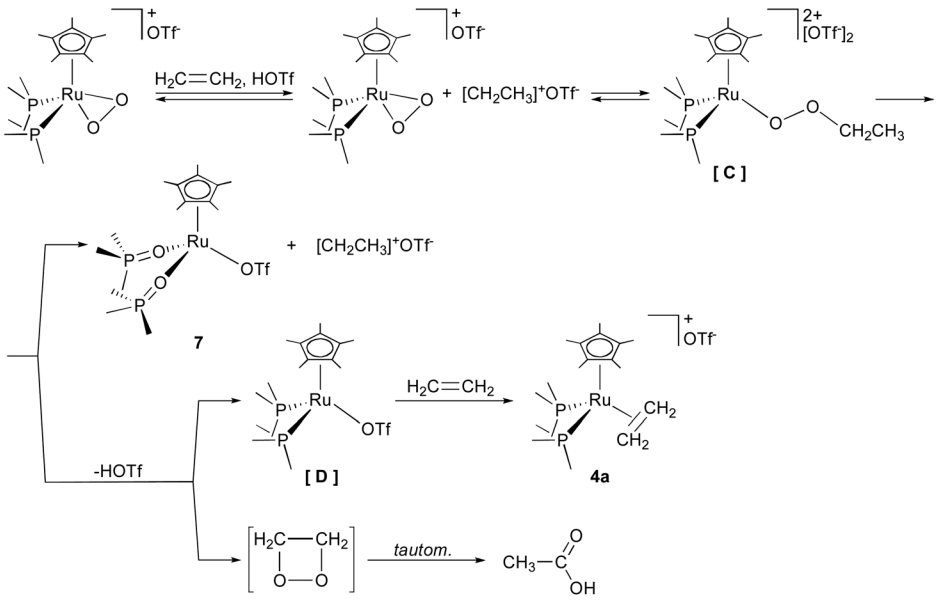

Scheme 8 Proposed reaction path. P = P(OEt)$_3$

Phosphate complexes [Ru(κ^1-OTf)(η^5-C_5Me_5){P(O)(OEt)$_3$}$_2$] (**7**) and [Ru(κ^1-OTf)(η^5-C_5Me_5){P(O)Ph$_3$}{P(O)(OMe)$_3$}] (**8**) were obtained as oils. However, the ^{1}H and ^{31}P NMR data support the proposed formulation showing, in the proton spectra, the signals of the η^5-C_5Me_5, of the phosphate P(O)(OEt)$_3$ and of the phosphine oxide P(O)Ph$_3$ ligands. In particular, a quintet at 4.27 and a triplet at 1.36 ppm appear in the proton spectra of **7**, due to the OCH_2CH_3 substituents of P(O)(OEt)$_3$, whereas the ^{31}P spectrum is a singlet at −2.77 ppm of the phosphate. Instead, in the ^{1}H NMR, a doublet at 3.89 ppm of P(O)(OMe)$_3$ is observed for **8**, whereas the ^{31}P spectrum shows a singlet at 30.5 ppm, attributed to P(O)Ph$_3$ and another at 0.47 ppm, due to P(O)(OMe)$_3$, fitting the proposed formulation.

Good analytical data were obtained for the tris(isocyanide) derivative [Ru(η^5-C_5Me_5)(^{t}BuNC)$_3$]BPh$_4$ (**9**), which was isolated as an orange solid stable in air and in solution of polar organic solvents, where it behaves as a 1 : 1 electrolyte.[11] Its IR spectrum shows two strong bands at 2175 and 2230 cm^{-1}, attributed to the ν_{CN} of the isocyanide ligands. The ^{1}H NMR spectrum supports the presence of the ^{t}BuNC ligands, showing a singlet at 1.48 ppm of the ^{t}Bu protons, while a singlet at 1.88 ppm is attributed to the methyl protons of the η^5-C_5Me_5, in agreement with the proposed formulation.

Conclusions

In this paper we report that dioxygen complexes **1–3**, stabilised by the half-sandwich fragment [Ru(η^5-C_5Me_5){P(OR)$_3$}L]$^+$ [L = P(OR)$_3$, PPh$_3$] undergo intramolecular oxygen transfer in the presence of acid, affording phosphate [Ru(κ^1-OTf)(η^5-C_5Me_5){P(O)(OEt)$_3$}$_2$] (**7**) and [Ru(κ^1-OTf)(η^5-C_5Me_5){P(O)Ph$_3$}{P(O)(OMe)$_3$}] (**8**) derivatives. Protonation of oxygen complexes under CH_2=CH_2 (1 atm) gives, besides phosphate, acetic acid.

Experimental

Materials and physical measurements

All synthetic work was carried out in an appropriate atmosphere (Ar, N_2) using standard Schlenk techniques or in an inert atmosphere dry-box. All solvents were dried over appropriate drying agents, degased on a vacuum line, and distilled into vacuum-tight storage flasks. $RuCl_3 \cdot 3H_2O$ was a Pressure Chemical Co. (USA) product, whereas pentamethylcyclopentadiene C_5Me_5H was a STREM (USA) product, used as received. Phosphites P(OMe)$_3$ and P(OEt)$_3$ and ^{t}butylisocyanide were Aldrich products used as received. Other reagents were purchased from commercial sources in the highest available purity and used as received. Infrared spectra were recorded on a PerkinElmer Spectrum-One FT-IR spectrophotometer. NMR spectra (^{1}H, ^{13}C, ^{31}P) were obtained on an AVANCE 300 Bruker spectrometer at temperatures between −90 and +25 °C, unless otherwise noted. ^{1}H and ^{13}C spectra are referred to internal tetramethylsilane. ^{31}P{^{1}H} chemical shifts are reported with respect to 85% H_3PO_4, with downfield shifts considered positive. COSY, HMQC and HMBC NMR experiments were performed with standard programs. The iNMR software package[17] was used to treat NMR data. The conductivity of 10^{-3} mol dm^{-3} solutions of the complexes in CH_3NO_2 at 25 °C was measured on a Radiometer CDM 83. Elemental analyses were determined in the Microanalytical Laboratory of the Dipartimento di Scienze del Farmaco, University of Padova (Italy).

Synthesis of the complexes

Pentamethylcyclopentadienyl complexes [RuCl(η^5-C_5Me_5){P(OEt)$_3$}$_2$] and [RuCl(η^5-C_5Me_5)(PPh$_3$){P(OR)$_3$}] (R = Me, Et) were prepared following the methods previously reported.[10b]

[Ru(η^5-C_5Me_5)(η^2-O_2){P(OEt)$_3$}$_2$]BPh$_4$ (1) and [Ru(η^5-C_5Me_5)(η^2-O_2)(PPh$_3$){P(OR)$_3$}]BPh$_4$ (2, 3) [R = Me (2), Et (3)]

In a 25 mL three-necked round-bottomed flask were placed 0.3 mmol of either the appropriate chloro compounds [RuCl(η^5-C_5Me_5){P(OEt)$_3$}$_2$] or [RuCl(η^5-C_5Me_5)(PPh$_3$){P(OR)$_3$}], an excess of NaBPh$_4$ (0.6 mmol, 205 mg), 10 mL of ethanol and 8 mL of dichloromethane. The resulting solution was allowed to stir under air (1 atm) at room temperature for 48 h. The solvent was removed under reduced pressure to give an oil, which was triturated with ethanol (2 mL) until a yellow solid separated out, which was filtered and crystallised from CH_2Cl_2 and EtOH; yield 85% (235 mg) for **1**, 79% (231 mg) for **2**, 81% (247 mg) for **3**.

1: IR (KBr, cm^{-1}) ν_{O-O} 935 (m); ^{1}H NMR (CD_2Cl_2, 20 °C) δ: 7.32–6.87 (m, 20H, Ph), 4.17 (m, 12H, CH_2), 1.70 (t, 15H, CH_3 Cp*), 1.35 (t, 18H, CH_3 phos); ^{31}P{^{1}H} NMR (CD_2Cl_2, 20 °C) δ: A_2 spin syst., 117.0 (s); Anal. calcd for $C_{46}H_{65}BO_8P_2Ru$ (919.83): C, 60.06; H, 7.12; found: C, 59.87; H, 7.19%; Λ_M = 52.6 Ω^{-1} mol^{-1} cm^2.

2: ^{1}H NMR (CD_2Cl_2, 20 °C) δ: 7.44–6.81 (m, 35H, Ph), 3.37 (d, 9H, CH_3 phos), 1.38 (dd, 15H, CH_3 Cp*); ^{31}P{^{1}H} NMR (CD_2Cl_2, 20 °C) δ: AX spin syst., δ_A 119.15, δ_X 36.2, J_{AX} = 90.41; Anal. calcd for $C_{55}H_{59}BO_5P_2Ru$ (973.88): C, 67.83; H, 6.11; found: C, 67.62; H, 6.04%; Λ_M = 53.2 Ω^{-1} mol^{-1} cm^2.

3: ^{1}H NMR (CD_2Cl_2, 20 °C) δ: 7.80–6.86 (m, 35H, Ph), 4.05 (qnt, 6H, CH_2), 1.43 (dd, 15H, CH_3 Cp*), 1.30 (t, 9H, CH_3 phos); ^{31}P{^{1}H} NMR (CD_2Cl_2, 20 °C) δ: AX spin syst., δ_A 113.9, δ_X 36.62, J_{AX} = 91.38; Anal. calcd for $C_{58}H_{65}BO_5P_2Ru$ (1015.96): C, 68.57; H, 6.45; found: C, 68.40; H, 6.57%; Λ_M = 54.1 Ω^{-1} mol^{-1} cm^2.

[Ru(η^5-C_5Me_5)(η^2-CH_2=CH_2){P(OEt)$_3$}L]BPh$_4$ (4) [L = P(OEt)$_3$ (a), PPh$_3$ (b)]

A solution of the appropriate dioxygen complex [Ru(η^5-C_5Me_5)(η^2-O_2){P(OEt)$_3$}L]BPh$_4$ (**1–3**) (0.11 mmol) in 10 mL of 1,2-dichloroethane was refluxed under ethylene (1 atm) for 1 h. The solvent was removed under reduced pressure to leave an oil, which was triturated with ethanol (1 mL). A yellow solid slowly separated out, which was filtered and crystallised from CH_2Cl_2 and EtOH; yield 87% (88 mg) for **4a**, 85% (95 mg) for **4b**.

4a: ^{1}H NMR (CD_2Cl_2, 20 °C) δ: 7.45–6.87 (m, 20H, Ph), 4.08 (m, 12H, CH_2 phos), 3.05 (t, 4H, CH_2=CH_2, J_{PH} = 3.5 Hz), 1.62 (s, 15H, CH_3 Cp*), 1.35 (t, 18H, CH_3 phos); ^{31}P{^{1}H} NMR (CD_2Cl_2, 20 °C) δ: A_2 spin syst., 131.5 (s); Anal. calcd for $C_{48}H_{69}BO_6P_2Ru$ (915.89): C, 62.95; H, 7.59; found: C, 63.13; H, 7.44%; Λ_M = 52.3 Ω^{-1} mol^{-1} cm^2.

4b: ^{1}H NMR (CD_2Cl_2, 20 °C) δ: 7.55–6.87 (m, 35H, Ph), 4.02 (m, 6H, CH_2 phos), ABCDXY spin syst. (ABCD = ^{1}H; X, Y = ^{31}P), δ_A = δ_B 2.48, δ_C = δ_D 2.31, J_{AB} = J_{CD} = 13.2, J_{AC} = J_{BD} = −1.00, J_{AD} = J_{BC} = 8.35, J_{AX} = J_{BX} = 5.50, J_{AY} = J_{BY} = 0.70, J_{CX} = J_{DX} = 5.50, J_{CY} = J_{DY} = 0.75 (4H, CH_2=CH_2), 1.42 (br, 15H, CH_3 Cp*), 1.29 (t, 9H, CH_3 phos); ^{31}P{^{1}H} NMR (CD_2Cl_2, 20 °C) δ: AX spin syst., δ_A 116.2, δ_X 42.5, J_{AX} = 52.3; Anal. calcd for $C_{60}H_{69}BO_3P_2Ru$ (1012.02): C, 71.21; H, 6.87; found: C, 71.04; H, 6.99%; Λ_M = 51.6 Ω^{-1} mol^{-1} cm^2.

[Ru(η^5-C_5Me_5)(η^2-ma){P(OEt)$_3$}$_2$]BPh$_4$ (5) and [Ru(η^5-C_5Me_5){=C=C(H)Ph}{P(OEt)$_3$}$_2$]BPh$_4$ (6) [ma = CH=CHCO(O)CO]

An excess (0.3 mmol) of the appropriate reagent CH=CHCO(O)CO (ma) (29 mg) or PhC≡CH (34 μL) was added to a solution of the dioxygen complex [Ru(η^5-C_5Me_5)(η^2-O_2){P(OEt)$_3$}$_2$]BPh$_4$ (**1**) (100 mg, 0.109 mmol) in 10 mL of 1,2-dichloroethane and the reaction mixture refluxed for 1 h. The solvent was removed under reduced pressure to give an oil, which was triturated with ethanol (1 mL). A yellow solid separated out, which was filtered and crystallised from CH_2Cl_2 and EtOH; yield 84% (90 mg) for **5**, 81% (87 mg) for **6**.

5: IR (KBr, cm^{-1}) ν_{CO} 1825, 1752 (s); ^{1}H NMR (CD_2Cl_2, 20 °C) δ: 7.35–6.86 (m, 20H, Ph), 4.12 (m, 12H, CH_2), 3.87 (t, 2H, =CH), 1.58 (br, 15H, CH_3 Cp*), 1.37 (t, 18H, CH_3 phos); ^{31}P{^{1}H} NMR (CD_2Cl_2, 20 °C) δ: A_2 spin syst., 130.0 (s); Anal. calcd for $C_{50}H_{67}BO_9P_2Ru$ (985.89): C, 60.91; H, 6.85; found: C, 60.76; H, 6.94%; Λ_M = 51.9 Ω^{-1} mol^{-1} cm^2.

6: IR (KBr, cm^{-1}) $\nu_{Ru=C=}$ 1646 (m); ^{1}H NMR (CD_2Cl_2, 20 °C) δ: 7.63–6.88 (m, 25H, Ph), 5.60 (t, 1H, =CH), 4.06 (m, 12H, CH_2), 1.88 (t, 15H, CH_3 Cp*), 1.31 (t, 18H, CH_3 phos); ^{31}P{^{1}H} NMR (CD_2Cl_2, 20 °C) δ: A_2 spin syst., 136.9 (s); ^{13}C NMR (CD_2Cl_2, 20 °C): 360.85 (t, J_{CP} = 18.5 Hz, Ru=C=), 165–122 (m, Ph), 116.29 (s, =CH), 104.84 (d, C_5 Cp*), 63.50 (t, OCH_2), 16.13 (t, CH_3 phos), 10.06 (s, CH_3 Cp*); Anal. calcd for $C_{54}H_{71}BO_6P_2Ru$ (989.97): C, 65.52; H, 7.23; found: C, 65.33; H, 7.19%; Λ_M = 52.5 Ω^{-1} mol^{-1} cm^2.

Protonation of [Ru(η^5-C_5Me_5)(η^2-O_2){P(OEt)$_3$}$_2$]BPh$_4$ (1) and [Ru(η^5-C_5Me_5)(η^2-O_2)(PPh$_3$){P(OMe)$_3$}]BPh$_4$ (2)

A solution of the appropriate dioxygen complex [Ru(η^5-C_5Me_5)(η^2-O_2){P(OEt)$_3$}$_2$]BPh$_4$ (**1**) or [Ru(η^5-C_5Me_5)(η^2-O_2)(PPh$_3$){P(OMe)$_3$}]BPh$_4$ (**2**) (0.02 mmol) in CD_2Cl_2 (1.0 mL), placed in a 5 mm NMR tube, was cooled to −30 °C and then one equivalent of HOTf (0.02 mmol, 1.8 μL) was added. The tube was introduced into the NMR probe, pre-cooled to −30 °C, and spectra recorded. Additional amounts of HOTf were added up to three equivalents and after each addition spectra recorded.

[Ru(κ^1-OTf)(η^5-C_5Me_5){P(O)(OEt)$_3$}$_2$] (7) and [Ru(κ^1-OTf)(η^5-C_5Me_5){P(O)Ph$_3$}{P(O)(OMe)$_3$}] (8)

An excess of triflic acid (0.33 mmol, 29 μL) was added to the solution of the appropriate dioxygen complex [Ru(η^5-C_5Me_5)(η^2-O_2){P(OEt)$_3$}$_2$]BPh$_4$ (**1**) or [Ru(η^5-C_5Me_5)(η^2-O_2)(PPh$_3$){P(OMe)$_3$}]BPh$_4$ (**2**) (0.11 mmol) in CH_2Cl_2 (10 mL) cooled to −80 °C. The reaction mixture was allowed to reach room temperature and stirred for 24 h. The solvent was removed under reduced pressure, leaving an oil which we were not able to separate as a solid.

7: ^{1}H NMR (CD_2Cl_2, 20 °C) δ: 4.27 (qnt, 12H, CH_2), 1.94 (br, 15H, CH_3 Cp*), 1.36 (t, 18H, CH_3 phos); $^{31}P\{^1H\}$ NMR (CD_2Cl_2, 20 °C) δ: A_2 spin syst., −2.77 (s); Λ_M = 4.2 Ω^{-1} mol^{-1} cm^2.

8: ^{1}H NMR (CD_2Cl_2, 20 °C) δ: 7.69–7.44 (m, 15H, Ph phos), 3.89 (d, 9H, CH_3 phos), 1.91 (s, 15H, CH_3 Cp*); $^{31}P\{^1H\}$ NMR (CD_2Cl_2, 20 °C) δ: A + A spin syst., 30.5 [s, $P(O)Ph_3$], 0.47 [s, $P(O)(OMe)_3$]; Λ_M = 3.9 Ω^{-1} mol^{-1} cm^2.

Preparation of [Ru(η^5-C_5Me_5)(^{t}BuNC)$_3$]BPh_4 (9) and separation of $P(O)(OEt)_3$

An excess of HOTf (0.6 mmol, 53 μL) was added to a solution of the dioxygen complex [Ru(η^5-C_5Me_5)(η^2-O_2){$P(OEt)_3$}$_2$]BPh_4 (**1**) (184 mg, 0.2 mmol) in 7 mL of dichloromethane, cooled to −80 °C. The reaction mixture was allowed to reach room temperature, stirred for 24 h, and then an excess of ^{t}butylisocyanide $(CH_3)_3CNC$ (1.0 mmol, 113 μL) added. After 2 h of stirring, the solvent was removed under reduced pressure to give an oil, which was triturated with ethanol (3 mL) containing an excess of $NaBPh_4$ (0.4 mmol, 137 mg). A yellow solid separated out, which was filtered and crystallised from CH_2Cl_2 and EtOH; yield 83% (134 mg).

The mother liquor was chromatographed on a silica gel column (60 cm) using petroleum ether 40–60 °C as eluent. The first eluted species was evaporated to dryness and characterised by ^{1}H and ^{31}P NMR spectra as $P(O)(OEt)_3$ (yield ≥ 75%).

It is worth noting that free $P(OEt)_3$ was not oxidised by air to $P(O)(OEt)_3$ under the same conditions used for the formation of **7**.

9: IR (KBr, cm^{-1}) ν_{CN} 2175 (m), 2130 (s); ^{1}H NMR (CD_2Cl_2, 20 °C) δ: 7.31–6.87 (m, 20H, Ph), 1.88 (s, 15H, CH_3 Cp*), 1.48 (s, 27H, CH_3 ^{t}Bu); Anal. calcd for $C_{49}H_{62}BN_3Ru$ (804.92): C, 73.12; H, 7.76; found: C, 72.95; H, 7.62%; Λ_M = 54.8 Ω^{-1} mol^{-1} cm^2.

$P(O)(OEt)_3$: ^{1}H NMR (CD_2Cl_2, 20 °C) δ: 4.04 (m, 6H, CH_2), 1.28 (t, 9H, CH_3); $^{31}P\{^1H\}$ NMR (CD_2Cl_2, 20 °C) δ: 0.81 ppm.

Separation of $P(O)(OMe)_3$ and $P(O)Ph_3$

The method was exactly like that used for precursor [Ru(η^5-C_5Me_5)(η^2-O_2){$P(OEt)_3$}$_2$]BPh_4 (**1**), but starting from the mixed-ligand derivative [Ru(η^5-C_5Me_5)(η^2-O_2)(PPh_3){$P(OMe)_3$}]BPh_4 (**2**). After separation of the tris(isocyanide) complex **9**, the mother liquor was chromatographed on a silica gel column (60 cm) using a mixture of petroleum ether 40–60 °C, dichloromethane and ethanol in 20 : 5 : 2 ratio as eluent. The first eluted species was evaporated to dryness and characterised as a mixture (ratio about 1 : 1) of $P(O)Ph_3$ and $P(O)(OMe)_3$ (yield ≥ 70%).

$P(O)(OMe)_3$: ^{1}H NMR ($CDCl_3$, 20 °C) δ: 3.76 (d, 9H, CH_3); $^{31}P\{^1H\}$ NMR ($CDCl_3$, 20 °C) δ: 2.6 ppm.

$P(O)Ph_3$: ^{1}H NMR ($CDCl_3$, 20 °C) δ: 7.78, 7.45 (m, 15H, Ph); $^{31}P\{^1H\}$ NMR ($CDCl_3$, 20 °C) δ: 29.6 ppm.

Protonation of [Ru(η^5-C_5Me_5)(η^2-O_2){$P(OEt)_3$}$_2$]BPh_4 (1) under CH_2=CH_2 atmosphere

A solution of the dioxygen complex **1** (92 mg, 0.1 mmol) in 5 mL of $CDCl_3$ was allowed to stand under a CH_2=CH_2 atmosphere (1 atm), cooled to −30 °C and treated with two equivalents of HOTf (0.2 mmol, 17.6 μL). The reaction mixture was left to reach room temperature and ^{1}H and ^{31}P NMR spectra recorded. ^{1}H NMR ($CDCl_3$, 20 °C) δ: 2.07 (s, 3H, CH_3 *HAc*).

Crystal structure determinations

Crystallographic data were collected in the CACTI (Universidade de Vigo) at low temperature using a Bruker D8 Venture with a CMOS Photon 100 detector and Mo-Kα radiation (λ = 0.71073 Å) equipped with a CryoStream 800 system. The software APEX3[18] was used for collecting frames of data, indexing reflections, and the determination of lattice parameters, SAINT[18] for integration of intensity of reflections, and SADABS[18] for scaling and empirical absorption correction. The crystallographic treatment was performed with the Oscail program[19] The structures of all the compounds were solved by using the SHELXT program[20] and refined by a full-matrix least-squares based on F^2, SHELXL program.[21] Non-hydrogen atoms were refined with anisotropic displacement parameters. Hydrogen atoms were included in idealised positions and refined with isotropic displacement parameters. For compound **3**, the Squeeze program[22] was used to eliminate the reflections due a disorder solvent. In addition, some disorder was found in one of the ethoxy groups in this compound. Details of crystal data and structural refinement are given in Table 2. CCDC 1842088–1842090† contain the supplementary crystallographic data for this paper.

Computational details

The geometry optimisations and energy calculations were carried out using the hybrid-GGA EDF2 functional[23] in combination with the 6-31G** basis set (ECP-based LANL2DZ basis set for Ru)[24] and the range-separated DFT functional ωB97X[25] in combination with the split-valence polarised basis set of Ahlrichs and Weigend, with Dolg's and co-workers ECP for the ruthenium centre.[26] The stationary points were characterised by vibrational analysis, from which zero-point vibrational energies and thermal corrections (T = 298.15 K) were obtained.[27] The implicit solvation model C-PCM (ε = 9.08) was used for ωB97X optimisations and EDF2 single point calculations.[28] The Gaussian 09 Program was used for ωB97X calculations,[29] the Spartan'16 Program for EDF2 calculations.[30] The software Multiwfn (version 3.3.8)[31] was used for Hirshfeld population analyses.[32]

Conflicts of interest

There are no conflicts of interest to declare.

Acknowledgements

The financial support of MIUR (Italy) – PRIN 2016 is gratefully acknowledged. We thank Daniela Baldan, from the Università Ca' Foscari Venezia (Italy), for technical assistance.

Table 2 Crystal data and structure refinement

Identification code	1	2	3
Empirical formula	$C_{46}H_{65}BO_8P_2Ru$	$C_{56}H_{61}BCl_2O_5P_2Ru$	$C_{58}H_{65}BO_5P_2Ru$
Moiety formula	$C_{22}H_{45}O_8P_2Ru$, $C_{24}H_{20}B$	$C_{31}H_{39}O_5P_2Ru$, $C_{24}H_{20}B$, CH_2Cl_2	$C_{34}H_{45}O_5P_2Ru$, $C_{24}H_{20}B$
Formula weight	919.80	1058.76	1015.92
Temperature (K)	100(2)	100(2)	100(2)
Wavelength (Å)	0.71073	0.71073	0.71073
Crystal system	Triclinic	Triclinic	Triclinic
Space group	$P\bar{1}$	$P\bar{1}$	$P\bar{1}$
Unit cell dimensions (a, b, c (Å))	a = 10.1044(7)	a = 12.8026(13)	a = 10.7189(9)
	b = 13.9566(11)	b = 13.4361(12)	b = 14.4422(13)
	c = 17.0124(13)	c = 16.0287(17)	c = 17.6629(16)
(α, β, γ (°))	α = 85.731(2)	α = 85.349(5)	α = 98.425(3)
	β = 77.016(2)	β = 84.245(5)	β = 102.113(3)
	γ = 83.628(2)	γ = 69.965(4)	γ = 90.545(3)
Volume (Å^3)	2320.3(3)	2574.1(4) Å^3	2642.3(4) Å^3
Z	2	2	2
Calc. ρ (Mg m^{-1})	1.317	1.366	1.277
μ (mm^{-1})	0.457	0.518	0.404
F(000)	968	1100	1064
Crystal size (mm)	0.174 × 0.102 × 0.095	0.085 × 0.053 × 0.048	0.211 × 0.142 × 0.063
Θ range (°)	2.460 to 28.372	2.204 to 28.426	2.364 to 28.458.
Index ranges	$-13 \le h \le 13$	$-17 \le h \le 17$	$-14 \le h \le 14$
	$-18 \le k \le 18$	$-17 \le k \le 17$	$-19 \le k \le 19$
	$-22 \le l \le 22$	$-21 \le l \le 21$	$-23 \le l \le 23$
Reflections collected	100 099	86 507	163 708
Independent reflections	11 590 [R(int) = 0.0267]	12 844 [R(int) = 0.0599]	13 230 [R_{int} = 0.0329]
Reflections observed (>2σ)	10 796	11 026	12 407
Data completeness	0.997	0.993	0.991
Absorption correction	Semi-empirical from equivalents		
Max. and min. transmission	0.7457 and 0.7242	0.7394 and 0.6994	0.7444 and 0.7206
Refinement method	Full-matrix least-squares on F^2		
Data/restraints/parameters	11 590/0/535	12 844/0/614	13 229/0/632
Goodness-of-fit on F^2	1.064	1.038	1.049
Final R indices [$I > 2\sigma(I)$]	R_1 = 0.0229	R_1 = 0.0417	R_1 = 0.0244
	wR_2 = 0.0586	wR_2 = 0.0922	wR_2 = 0.0618
R indices (all data)	R_1 = 0.0259	R_1 = 0.0532	R_1 = 0.0280
	wR_2 = 0.0600	wR_2 = 0.0970	wR_2 = 0.0635
Largest diff. peak and hole (e Å^{-3})	0.373 and −0.556	2.034 and −2.269	0.476 and −0.505

References

1 (*a*) *Active Oxygen in Biochemistry*, ed. J. S. Valentine, C. S. Foote, A. Greenberg and J. F. Liebman, Blackie Academic and Professional, London, UK, 1995; (*b*) L. Que and R. Y. N. Ho, *Chem. Rev.*, 1996, **96**, 2607–2624; (*c*) B. J. Wallar and J. D. Lipscomb, *Chem. Rev.*, 1996, **96**, 2625–2658; (*d*) M. Sono, M. P. Roach, E. D. Coulter and J. H. Dawson, *Chem. Rev.*, 1996, **96**, 2841–2888; (*e*) V. R. I. Kaila, M. I. Verkhovsky and M. Wikström, *Chem. Rev.*, 2010, **110**, 7062–7081; (*f*) E. I. Solomon, P. Chen, M. Metz, S.-K. Lee and A. E. Palmer, *Angew. Chem.*, 2001, **113**, 4702–4724, (*Angew. Chem., Int. Ed.*, 2001, **40**, 4570–4590); (*g*) I. G. Denisov, T. M. Makris, S. G. Sligar and I. Schlichting, *Chem. Rev.*, 2005, **105**, 2253–2278.

2 (*a*) A. S. Matlack, *Introduction to Green Chemistry*, Marcel Dekker, New York, USA, 2001; (*b*) S. S. Stahl, *Angew. Chem.*, 2004, **116**, 3480–3501, (*Angew. Chem., Int. Ed.*, 2004, **43**, 3400–3420); (*c*) S. S. Stahl, *Science*, 2005, **309**, 1824–1826; (*d*) *The Activation of Dioxygen and Homogeneous Catalytic Oxidation*, ed. D. H. R. Barton, A. E. Martell and D. T. Sawyer, Plenum, London, New York, USA, 1993; (*e*) B. R. James, *Dioxygen Activation and Homogeneous Catalytic Oxidation*, ed. L. I. Simàndi, Elsevier, Amsterdam, NL, 1991, p. 195; (*f*) H. Mimoun, *Angew. Chem., Int. Ed. Engl.*, 1982, **21**, 734–750; (*g*) H. Mimoun, *Pure Appl. Chem.*, 1981, **53**, 2389–2399; (*h*) R. A. F. Tomas, J. C. M. Bordado and J. F. P. Gomes, *Chem. Rev.*, 2013, **113**, 7421–7469; (*i*) L. Boisvert and K. I. Goldberg, *Acc. Chem. Res.*, 2012, **45**, 899–910; (*j*) Z. Shi, C. Zhang, C. Tang and N. Jiao, *Chem. Soc. Rev.*, 2012, **41**, 3381–3430.

3 (*a*) W. A. Nugent and J. M. Mayer, *Metal-Ligand Multiple Bonds*, Wiley, New York, USA, 1988; (*b*) D. W. Pipes and T. J. Meyer, *Inorg. Chem.*, 1986, **25**, 4042–4050; (*c*) C. M. Che, T. F. Lai and K. Y. Wong, *Inorg. Chem.*, 1987, **26**, 2289–2299; (*d*) M. E. Marmion and K. J. Takeuchi, *J. Am. Chem. Soc.*, 1988, **110**, 1472–1480; (*e*) C. M. Che, W. K. Cheng and V. W. W. Yam, *J. Chem. Soc., Dalton Trans.*, 1990, 3095–3100; (*f*) M. Bourgault, A. Castillo, M. A. Esteruelas, E. Oñate and N. Ruiz, *Organometallics*, 1997, **16**, 636–645; (*g*) H. Molina-Svendsen, G. Bojesen and C. J. McKenzie, *Inorg. Chem.*, 1998, **37**, 1981–1983; (*h*) M. J. Camenzind, B. R. James and D. Dolphin, *J. Chem. Soc., Chem. Commun.*, 1986, 1137–1139; (*i*) D. K. Dogutan,

S. A. Stoian, R. McGuire, M. Schwalbe, T. S. Teets and D. G. Nocera, *J. Am. Chem. Soc.*, 2011, **133**, 131–140; (*j*) J. Y. Yang, R. M. Bullock, W. G. Dougherty, W. S. Kassel, B. Twamley, D. L. DuBois and M. Rakowski DuBois, *Dalton Trans.*, 2010, **39**, 3001–3010; (*k*) R. L. Shook, S. M. Peterson, J. Greaves, C. Moore, A. L. Rheingold and A. S. Borovik, *J. Am. Chem. Soc.*, 2011, **133**, 5810–5817.

4 (*a*) A. Sen and J. Halpern, *J. Am. Chem. Soc.*, 1977, **99**, 8337–8339; (*b*) A. van Asselt, M. S. Trimmer, L. M. Henling and J. E. Bercaw, *J. Am. Chem. Soc.*, 1988, **110**, 8254–8255; (*c*) S. Bhaduri, L. Casella, R. Ugo, P. R. Raithby, C. Zuccaro and M. B. Hursthouse, *J. Chem. Soc., Dalton Trans.*, 1979, 1624–1628; (*d*) K. Kirchner, K. Mauthner, K. Mereiter and R. Schmid, *J. Chem. Soc., Chem. Commun.*, 1993, 892–894; (*e*) K. Mauthner, K. Mereiter, R. Schmid and K. Kirchner, *Inorg. Chim. Acta*, 1995, **236**, 95–100; (*f*) M. Sato and M. Asai, *J. Organomet. Chem.*, 1996, **508**, 121–127; (*g*) E. Lindner, M. Haustein, R. Fawzi, M. Steimann and P. Wagner, *Organometallics*, 1994, **13**, 5021–5029; (*h*) S. M. Maddock, C. E. F. Rickard, W. R. Roper and L. James Wright, *J. Organomet. Chem.*, 1996, **510**, 267–279; (*i*) I. de los Ríos, M. Jiménez Tenorio, J. Padilla, M. C. Puerta and P. Valerga, *Organometallics*, 1996, **15**, 4565–4574; (*j*) T. Y. Bartucz, a. Golombek, A. J. Lough, P. A. Maltby, R. H. Morris, R. Ramachandran and M. Schlaf, *Inorg. Chem.*, 1998, **37**, 1555–1562; (*k*) P. Barthazy, M. Wörle and A. Mezzetti, *J. Am. Chem. Soc.*, 1999, **121**, 480–481; (*l*) G. Jia, W. S. Ng, H. S. Chu, W.-T. Wong, N.-T. Yu and I. D. Williams, *Organometallics*, 1999, **18**, 3597–3602; (*m*) H. Yu, Y. Fu, Q. Guo and Z. Lin, *Organometallics*, 2009, **28**, 4443–4451; (*n*) P. Barthazy, M. Wörle, H. Rüegger and A. Mezzetti, *Inorg. Chem.*, 2000, **39**, 4903–4912; (*o*) M. E. Navarro Clemente, P. J. Saavedra, M. Cervantes Vásquez, M. A. Paz-Sandoval, A. M. Arif and R. D. Ernst, *Organometallics*, 2002, **21**, 592–605; (*p*) K. Fujita, R. Schenker, W. Gu, T. C. Brunold, S. P. Cramer and C. G. Riordan, *Inorg. Chem.*, 2004, **43**, 3324–3326; (*q*) J. Matthes, S. Gründemann, A. Toner, Y. Guari, B. Donnadieu, J. Spandl, S. Sabo-Etienne, E. Clot, H.-H. Limbach and B. Chaudret, *Organometallics*, 2004, **23**, 1424–1433; (*r*) L. Cuesta, E. Tomat, V. M. Lynch and J. L. Sessler, *Chem. Commun.*, 2008, 3744–3746; (*s*) W. M. Khairul, M. A. Fox, N. N. Zaitseva, M. Gaudio, D. S. Yufit, B. W. Skelton, A. H. White, J. A. K. Howard, M. I. Bruce and P. J. Low, *Dalton Trans.*, 2009, 610–620; (*t*) T. A. Tronic, M. R. DuBois, W. Kaminsky, M. K. Coggins, T. Liu and J. M. Mayer, *Angew. Chem., Int. Ed.*, 2011, **50**, 10936–10939.

5 (*a*) S. L. Kuan, W. K. Leong, R. D. Webster and L. Y. Goh, *Organometallics*, 2012, **31**, 5159–5168; (*b*) A. Yoshinari, A. Tazawa, S. Kuwata and T. Ikariya, *Chem. – Asian J.*, 2012, **7**, 1417–1425; (*c*) J. Cho, R. Sarangi and W. Nam, *Acc. Chem. Res.*, 2012, **45**, 1321–1330; (*d*) T. A. Tronic, W. Kaminsky, M. K. Coggins and J. M. Mayer, *Inorg. Chem.*, 2012, **51**, 10916–10928; (*e*) F. Avenier, C. Herrero, W. Leibl, A. Desbois, R. Guillot, J.-P. Mahy and A. Aukauloo, *Angew. Chem., Int. Ed.*, 2013, **52**, 3634–3637; (*f*) D. Munz and T. Strassner, *Inorg. Chem.*, 2015, **54**, 5043–5052; (*g*) T. Ishizuka, S. Ohzu and T. Kojima, *Synlett*, 2014, 1667–1679; (*h*) K. Gogoi, S. Saha, B. Mondal, H. Deka, S. Ghosh and B. Mondal, *Inorg. Chem.*, 2017, **56**, 14438–14445; (*i*) T. Bolaño, M. A. Esteruelas, M. P. Gay, E. Oñate, I. M. Pastor and M. Yus, *Organometallics*, 2015, **34**, 3902–3908.

6 (*a*) J. C. Dobson, W. K. Seok and T. J. Meyer, *Inorg. Chem.*, 1986, **25**, 1513–1514; (*b*) C. M. Che, C. K. Li, W. T. Tang and W. Y. Yu, *J. Chem. Soc., Dalton Trans.*, 1992, 3153–3158; (*c*) A. S. Goldstein, R. H. Beer and R. S. Drago, *J. Am. Chem. Soc.*, 1994, **116**, 2424–2429; (*d*) L. K. Stultz, R. A. Binstead, M. S. Reynolds and T. J. Meyer, *J. Am. Chem. Soc.*, 1995, **117**, 2520–2532; (*e*) T. S. Lai, H. L. Kwong, R. Zhang and C. M. Che, *J. Chem. Soc., Dalton Trans.*, 1998, 3559–3564.

7 (*a*) J. T. Groves and T. E. Nemo, *J. Am. Chem. Soc.*, 1983, **105**, 6243–6248; (*b*) A. S. Goldstein and R. S. Drago, *J. Chem. Soc., Chem. Commun.*, 1991, 21–22; (*c*) A. J. Bailey, W. P. Griffith and P. D. Savage, *J. Chem. Soc., Dalton Trans.*, 1995, 3537–3542.

8 (*a*) G. Albertin, S. Antoniutti, F. Callegaro and J. Castro, *Organometallics*, 2009, **28**, 4475–4479; (*b*) G. Albertin, S. Antoniutti, J. Castro and S. Paganelli, *J. Organomet. Chem.*, 2010, **695**, 2142–2152; (*c*) G. Albertin, S. Antoniutti, J. Castro and S. García-Fontán, *Eur. J. Inorg. Chem.*, 2011, 510–520; (*d*) G. Albertin, S. Antoniutti, J. Castro and S. Da Lio, *Organometallics*, 2013, **32**, 3651–3661; (*e*) G. Albertin, S. Antoniutti, J. Castro and F. Scapinello, *J. Organomet. Chem.*, 2014, **751**, 412–419; (*f*) G. Albertin, S. Antoniutti, M. Bortoluzzi, A. Botter and J. Castro, *Dalton Trans.*, 2015, **44**, 3439–3446; (*g*) G. Albertin, S. Antoniutti, M. Bortoluzzi, A. Botter and J. Castro, *Dalton Trans.*, 2015, **44**, 7411–7418.

9 (*a*) G. Albertin, S. Antoniutti, D. Baldan, J. Castro and G. Comparin, *Organometallics*, 2013, **32**, 3157–3160; (*b*) G. Albertin, S. Antoniutti, A. Botter, J. Castro and M. Giacomello, *Organometallics*, 2014, **33**, 3570–3582; (*c*) G. Albertin, S. Antoniutti, J. Castro and G. Dottorello, *Dalton Trans.*, 2015, **44**, 9289–9303; (*d*) G. Albertin, S. Antoniutti, M. Bortoluzzi, J. Castro and L. Marzaro, *Dalton Trans.*, 2015, **44**, 15470–15480; (*e*) G. Albertin, S. Antoniutti, M. Bortoluzzi, A. Botter, J. Castro and F. Sibilla, *RSC Adv.*, 2016, **6**, 97650–97658.

10 (*a*) G. Albertin, S. Antoniutti, A. Botter and J. Castro, *Inorg. Chem.*, 2015, **54**, 2091–2093; (*b*) G. Albertin, S. Antoniutti, M. Bortoluzzi, A. Botter and J. Castro, *Inorg. Chem.*, 2016, **55**, 5592–5602; (*c*) G. Albertin, S. Antoniutti, M. Bortoluzzi, A. Botter and J. Castro, *J. Organomet. Chem.*, 2016, **822**, 259–268.

11 W. J. Geary, *Coord. Chem. Rev.*, 1971, **7**, 81–122.

12 (*a*) L. J. Farrugia, *J. Appl. Crystallogr.*, 1997, **30**, 565; (*b*) *POV-Ray, v. 3.7 for Windows*, Persistence of Vision Pty. Ltd., 2016 Persistence of Vision Raytracer (Version 3.7).

13 A. Y. Kostukovich, D. I. D'yachihin, F. M. Dolgushin, A. F. Smolyakov, I. A. Godovikov and I. T. Chizhevsky, *Molecules*, 2014, **19**, 7094–7103.

14 M. D. Palacios, M. C. Puerta, P. Valerga, A. Lledós and E. Veilly, *Inorg. Chem.*, 2007, **46**, 6958–6967.
15 I. de los Ríos, M. Jiménez Tenorio, J. Padilla, M. C. Puerta and P. Valerga, *J. Chem. Soc., Dalton Trans.*, 1996, 377–381.
16 (*a*) H. Mimoun, M. M. Perez-Machirant and J. Seree de Roch, *J. Am. Chem. Soc.*, 1978, **100**, 5437–5444; (*b*) V. Conte, F. Di Furia and S. Moro, *J. Mol. Catal. A: Chem.*, 1997, **120**, 93–99; (*c*) M. Aresta, I. Tommasi, E. Quaranta, C. Fragale, J. Mascetti, m. Tranquille, F. Galan and M. Fouassier, *Inorg. Chem.*, 1996, **35**, 4254–4260; (*d*) H. Suzuki, S. Matsuura, Y. Moro-Oka and I. Ikawa, *J. Organomet. Chem.*, 1985, **286**, 247–258.
17 G. Balacco, http: //www.inmr.net/.
18 Bruker, *APEX3, SMART, SAINT*, Bruker AXS Inc., Madison, Wisconsin, USA, 2015.
19 P. McArdle, K. Gilligan, D. Cunningham, R. Dark and M. Mahon, *CrystEngComm*, 2004, **6**, 303–309.
20 G. M. Sheldrick, *Acta Crystallogr., Sect. A: Found. Adv.*, 2015, **71**, 3–8.
21 G. M. Sheldrick, *Acta Crystallogr., Sect. C: Struct. Chem.*, 2015, **71**, 3–8.
22 A. L. Spek, *Acta Crystallogr., Sect. C: Struct. Chem.*, 2015, **71**, 9–18.
23 C. Y. Lin, M. W. George and P. M. W. Gill, *Aust. J. Chem.*, 2004, **57**, 365–370.
24 (*a*) M. Dolg, *Modern methods and algorithms of quantum chemistry*, ed. J. Grotendorst, John Neumann Institute for Computing, NIC Series, Jülich, 2000, vol. 1, p. 479; (*b*) P. J. Hay and W. R. Wadt, *J. Chem. Phys.*, 1985, **82**, 270–283; (*c*) P. J. Hay and W. R. Wadt, *J. Chem. Phys.*, 1985, **82**, 299–310; (*d*) W. J. Henre, R. Ditchfield and J. A. Pople, *J. Chem. Phys.*, 1972, **56**, 2257–2261.
25 (*a*) Y. Minenkov, Å. Singstad, G. Occhipinti and V. R. Jensen, *Dalton Trans.*, 2012, **41**, 5526–5541; (*b*) J.-D. Chai and M. Head-Gordon, *Phys. Chem. Chem. Phys.*, 2008, **10**, 6615–6620; (*c*) I. C. Gerber and J. G. Ángyán, *Chem. Phys. Lett.*, 2005, **415**, 100–105.
26 (*a*) F. Weigend and R. Ahlrichs, *Phys. Chem. Chem. Phys.*, 2005, **7**, 3297–3305; (*b*) D. Andrae, U. Haussermann, M. Dolg, H. Stoll and H. Preuss, *Theor. Chim. Acta*, 1990, **77**, 123–141.
27 C. J. Cramer, *Essentials of Computational Chemistry*, Wiley, Chichester, 2nd edn, 2004.
28 (*a*) M. Cossi, N. Rega, G. Scalmani and V. Barone, *J. Comput. Chem.*, 2003, **24**, 669–681; (*b*) V. Barone and M. Cossi, *J. Phys. Chem. A*, 1998, **102**, 1995–2001.
29 M. J. Frisch, *et al.*, *Gaussian 09, Revision C.01*, Gaussian Inc., Wallingford CT, USA, 2010.
30 (*a*) *Spartan '16, Build 1.1.0*, Wavefunction Inc., Irvine CA, USA, 2016; (*b*) Y. Shao, *et al.*, *Mol. Phys.*, 2015, **113**, 184–215.
31 T. Lu and F. Chen, *J. Comput. Chem.*, 2012, **33**, 580–592.
32 F. L. Hirshfeld, *Theor. Chim. Acta*, 1977, **44**, 129–138.

